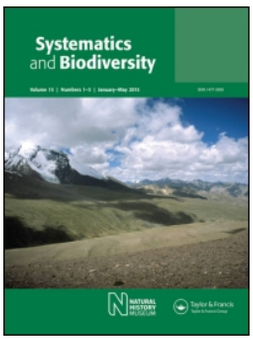

Systematics and Biodiversity

ISSN: 1477-2000 (Print) 1478-0933 (Online) Journal homepage: https://www.tandfonline.com/loi/tsab20

Integrative taxonomy reveals a new species of freshwater mussel, *Potamilus streckersoni* sp. nov. (Bivalvia: Unionidae): implications for conservation and management

Chase H. Smith, Nathan A. Johnson, Kentaro Inoue, Robert D. Doyle & Charles R. Randklev

To cite this article: Chase H. Smith, Nathan A. Johnson, Kentaro Inoue, Robert D. Doyle & Charles R. Randklev (2019): Integrative taxonomy reveals a new species of freshwater mussel, *Potamilus streckersoni* sp. nov. (Bivalvia: Unionidae): implications for conservation and management, Systematics and Biodiversity, DOI: 10.1080/14772000.2019.1607615

To link to this article: https://doi.org/10.1080/14772000.2019.1607615

Systematics and Biodiversity (2019), **0(0)**: 1–18

Taylor & Francis
Taylor & Francis Group

Research Article

Integrative taxonomy reveals a new species of freshwater mussel, *Potamilus streckersoni* sp. nov. (Bivalvia: Unionidae): implications for conservation and management

CHASE H. SMITH[1,2], NATHAN A. JOHNSON[2], KENTARO INOUE[3], ROBERT D. DOYLE[1] AND CHARLES R. RANDKLEV[3]

[1]Biology Department, Baylor University, Waco, TX, 76798, USA
[2]US Geological Survey, Wetland and Aquatic Research Center, 7920 NW 71st Street, Gainesville, FL, 32653, USA
[3]Texas A&M Natural Resources Institute, Texas A&M AgriLife Research Center at Dallas, Dallas, TX, 75252, USA

(Received 28 September 2018; accepted 10 March 2019)

Inaccurate systematics confound our ability to determine evolutionary processes that have led to the diversification of many taxa. The North American freshwater mussel tribe Lampsilini is one of the better-studied groups in Unionidae, however, many supraspecific relationships between lampsiline genera remain unresolved. Two genera previously hypothesized to be non-monophyletic that have been largely overlooked are *Leptodea* and *Potamilus*. We set out to resolve supraspecific relationships in Lampsilini and test the monophyly of *Leptodea* and *Potamilus* by integrating molecular, morphological, and life history data. Our molecular matrix consisted of four loci: *cytochrome c oxidase subunit 1* (CO1), *NADH dehydrogenase subunit 1* (ND1), *internal transcribed spacer 1* (ITS1), and *28S ribosomal RNA*. Secondly, we performed both traditional and Fourier shape morphometric analyses to evaluate morphological differences and finally, we compared our results with available life history data. Molecular data supported the paraphyly of both *Leptodea* and *Potamilus*, but nodal support was insufficient to make any conclusions regarding generic-level assignments at this time. In contrast, inference from our integrative taxonomic assessment depicts significant support for the recognition of a new species, *Potamilus streckersoni* sp. nov., the Brazos Heelsplitter. Our data show clear separation of three taxonomic entities in the *P. ohiensis* species complex: *P. amphichaenus*, *P. ohiensis*, and *P. streckersoni* sp. nov.; all molecularly, geographically, and morphologically diagnosable. Our findings have profound implications for unionid taxonomy and will aid stakeholders in establishing effective conservation and management strategies.

http://www.zoobank.org/urn:lsid:zoobank.org:pub:502647C0-418B-4CC4-85A8-BD89FC3F674F

Key words: Brazos Heelsplitter, imperilled species, Lampsilini, Leptodea, phylogenetics, species delimitation

Introduction

Inaccurate systematics continue to be a fundamental problem that confounds our ability to determine evolutionary processes that lead to the diversification of taxa (Johnson et al., 2018; Perkins, Johnson, & Gangloff, 2017; Pfeiffer, Johnson, Randklev, Howells, & Williams, 2016; Satler, Carstens, & Hedin, 2013; Smith, Johnson, Pfeiffer, & Gangloff, 2018). Unionid bivalves (Bivalvia: Unionidae) represent the most species-rich taxonomic group in the order Unionida, with over 650 recognized species (Graf & Cummings, 2007; Lopes-Lima et al., 2018). The unique life cycle of unionids, which involves parasitic larvae (glochidia) that must attach to vertebrate hosts prior to becoming sessile adults, has likely contributed significantly to the rampant diversification of this group (e.g., Barnhart, Haag, & Roston, 2008). This complex life cycle creates a unique co-evolutionary system, as freshwater mussels continually adapt to successfully infect their hosts.

Taxonomy in Unionidae has been particularly unstable and recent studies using molecular data have revealed cases of convergent evolution, cryptic diversity, inaccurate supraspecific relationships, and overestimated diversity at the species level (Inoue, Hayes, Harris, &

Correspondence to: Nathan A. Johnson. E-mail: najohnson@usgs.gov or Chase H. Smith. E-mail: Chase_Smith1@baylor.edu

ISSN 1477-2000 print / 1478-0933 online

https://dx.doi.org/10.1080/14772000.2019.1607615
Published online 03 Jul 2019

Christian, 2013; Johnson et al., 2018; Perkins et al., 2017; Pfeiffer et al., 2016; Smith et al., 2018; Williams et al., 2017). The freshwater mussel tribe Lampsilini Ihering, 1901 exhibits a wide diversity of host infection strategies unique to the Unionidae (Barnhart et al., 2008; Graf, 2013; Zanatta & Murphy, 2006) and has been the subject of many taxonomic studies. These previous studies primarily focused on the species-rich genus *Lampsilis* Rafinesque, 1820 and supraspecific relationships between many lampsiline genera remain unresolved. Two genera that have been largely overlooked are *Leptodea* Rafinesque, 1820 and *Potamilus* Rafinesque, 1818 which consist of 10 species endemic to the USA and Canada including several imperilled taxa (Williams et al., 2017). *Leptodea* and *Potamilus* have been considered closely related due to similar adult morphology, larval hosts, and habitat preference (Barnhart et al., 2008; Haag, 2012; Hoggarth, 1999; Sietman, Hove, & Davis, 2018); however, *Leptodea* and *Potamilus* have been classified as distinct genera based on differing glochidial morphologies (Barnhart et al., 2008; Hoggarth, 1999; Watters, Hoggarth, & Stansbery, 2009; Williams et al., 2017). Considering the strong selective pressures against parasitism, glochidial morphology is thought to be highly conserved and considered one of the most useful morphological characters in reconstructing the evolutionary history of freshwater mussels (Barnhart et al., 2008; Graf & Cummings, 2006; Haag, 2012; Hoggarth, 1999; Hoggarth & Gaunt, 1988; Williams, Butler, Warren, & Johnson, 2014). However, a previous phylogenetic assessment showed polyphyly of *Leptodea* and *Potamilus*, indicating that glochidial morphology may not be diagnostic for the two genera (Roe & Lydeard, 1998).

Concomitant to questionable monophyly at the generic-level, species in the genus *Potamilus* depict disjunct distributional patterns and high levels of intraspecific variation in shell morphology. For instance, *P. ohiensis* (Rafinesque, 1820) occurs throughout much of the Mississippi River Basin including the Red, Sulphur, and Cypress rivers in northern Texas, as well as a disjunct population in the Brazos River drainage in Texas (Howells, Neck, & Murray, 1996; Williams, Bogan, & Garner, 2008). This biogeographic pattern is unique within freshwater mussels, as no other unionid species is distributed only in the Mississippi and Brazos River drainages (Haag, 2009; Howells et al., 1996). Furthermore, shell morphology of *P. ohiensis* individuals from the Brazos River resembles that of *P. amphichaenus* (Frierson, 1898), a congener endemic to the Sabine, Neches, and Trinity River drainages in eastern Texas (Howells et al., 1996). This morphological similarity of *P. amphichaenus* and *P. ohiensis* from the Brazos River has led to speculation that *P. ohiensis* had been introduced into the Trinity River drainage (Howells et al., 1996). However, this hypothesis has not been validated using molecular techniques. The possibility of a syntopic form of *P. ohiensis* with *P. amphichaenus* is troubling, especially considering *P. amphichaenus* is petitioned for listing under the Endangered Species Act (USFWS, 2009) and a recent phylogenetic study revealed multiple morphologically cryptic sympatric species of *Fusconaia* Simpson, 1900 in the Trinity River (Pieri et al., 2018).

Previous studies evaluating phylogenetic relationships between *Leptodea* and *Potamilus* implemented a single locus coupled with limited sample sizes and incomplete taxon sampling (Roe & Lydeard, 1998). Although phylogenetic reconstruction based on a single locus has been conducted in recent freshwater mussels studies (Inoue et al., 2018), this methodology has been criticized due to the significant increase in accuracy when analysing loci from both nuclear and mitochondrial genomes (Fujita, Leaché, Burbrink, McGuire, & Moritz, 2012; Yang & Rannala, 2010; Zhang, Zhang, Zhu, & Yang, 2011). Phylogenetic inference from limited sampling has also been well-documented to greatly increase phylogenetic estimation error (Hillis, Pollock, McGuire, & Zwickl, 2003; Pollock, Zwickl, McGuire, & Hillis, 2002; Zwickl & Hillis, 2002); thus, proper sampling should be implemented before taxonomic recommendations are warranted. In this study, we present a robust multi-locus approach based on extensive taxonomic sampling to investigate supraspecific relationships between the genera *Leptodea* and *Potamilus*. We also investigate species-level diversity in *Potamilus* and implement an integrative taxonomic approach to resolve species boundaries and distributional patterns in the *P. ohiensis* species complex (*P. amphichaenus*, *P. ohiensis* from the Brazos River, and *P. ohiensis* from the Mississippi River Basin). We collect and analyse multiple independent lines of evidence, all of which support the recognition of three evolutionarily divergent groups within the *P. ohiensis* species complex: *P. amphichaenus* (Sabine, Neches, and Trinity rivers), *P. ohiensis* (Mississippi River Basin), and *P. ohiensis* endemic to the Brazos River. Below we present significant molecular, morphological, and biogeographic evidence that species-level diversity in this group was previously underestimated and we formally describe *Potamilus streckersoni* sp. nov., which is endemic to the Brazos River drainage in Texas.

Materials and methods

Taxon sampling and molecular data generation

To test the phylogenetic placement of *Leptodea* and *Potamilus*, we sampled material for North American

genera in the tribes Lampsilini, Amblemini Rafinesque, 1820, and additional material from Ambleminae *incertae sedis* (Williams et al., 2017). We focused our sampling on type species of each genus and type locality (Table S1, see online supplemental material, which is available from the article's Taylor & Francis Online page at http://dx.doi.org/10.1080/14772000.2019.1607615). We selected *Quadrula quadrula* (Rafinesque, 1820) to root our phylogeny following findings of tribe relationships in a previous study (Lopes-Lima et al., 2017). We sequenced two mitochondrial genes and two nuclear loci: a partial portion of *cytochrome c oxidase subunit 1* (CO1), *NADH dehydrogenase subunit 1* (ND1), the nuclear-encoded *ribosomal internal transcribed spacer 1* (ITS1), and a portion of the large ribosomal subunit *28S*. Mantle tissue samples were taken for DNA extraction either directly after specimens were euthanized or from samples preserved in 95% ethanol. Genomic DNA was extracted using the PureGene DNA extraction kit with the standard extraction protocol (Gentra Systems, Inc., Minneapolis, MN, USA). Primers used for polymerase chain reaction (PCR) and sequencing were: CO1 5′-GTTCCACAAATCATAAGGATATTGG-3′ and 5′-TACACCTCAGGGTGACCAAAAAACCA-3′ (Campbell et al., 2005); ND1 5′-TGGCAGAAAA GTGCATCAGATTAAAGC-3′ and 5′-CCTGCTTGGA AGGCAAGTGTACT-3′ (Serb, Buhay, & Lydeard, 2003); ITS1 5′-AAAAAGCTTCCGTAGGTGAACCT GCG-3′ and 5′-AGCTTGCTGCGTTCTTCATCG-3′ (King, Eackles, Gjetvaj, & Hoeh, 1999); 28S 5′-GGGACTACCCCCTGAATTTAAGCAT-3′ and 5′-CCA GCTATCCTGAGGGAAACTTCG-3′ (Park & Foighil, 2000). Thermal cycling conditions for CO1 followed Johnson et al. (2018), while all other conditions are given in King et al. (1999), Park & Foighil (2000), and Serb et al. (2003). PCR plate amplifications were conducted using a 12.5 µl mixture of the following: molecular grade water (4.25 µl), MyTaq^{TM} Red Mix (6.25 µl) (Bioline), primers (0.5 µl each), and DNA template (50 ng). PCR products were sent to the Molecular Cloning Laboratories (MCLAB, South San Francisco, CA, USA) for bi-directional sequencing on an ABI 3730. All ITS1 sequences were readable without cloning, similar to recent studies in unionids (Johnson et al., 2018; Pfeiffer et al., 2016; Pieri et al., 2018; Smith et al., 2018). Geneious v 10.2.3 was used to assemble contigs and edit chromatograms (Kearse et al., 2012) and sequences were aligned in Mesquite v 3.31 (Maddison & Maddison, 2017) using MAFFT v 7.311 (Katoh & Standley, 2013). The protein-coding genes (CO1 and ND1) were aligned using the L-INS-i method in MAFFT and translated into amino acids to ensure absence of stop codons and gaps. The ITS1 and 28S sequences were aligned using the E-INS-i method in MAFFT to better account for indels.

Phylogenetic reconstruction

We created a 4-locus concatenated dataset of CO1, ND1, ITS1, and 28S to estimate a phylogeny of Lampsilini using both Maximum likelihood (ML) and Bayesian inference (BI). Before phylogenetic inference was performed, we tested for nucleotide saturation in the three codon positions for protein-coding mitochondrial markers (i.e., CO1 and ND1) using the Xia test in Dambe v 7.0.35 (Xia, 2018; Xia, Xie, Salemi, Chen, & Wang, 2003). ML and BI analyses were subsequently performed in IQ-TREE v 1.6.6 (Chernomor, von Haeseler, & Minh, 2016; Nguyen, Schmidt, von Haeseler, & Minh, 2015) and MrBayes v 3.2.6 (Ronquist et al., 2012), respectively. We used ModelFinder (Kalyaanamoorthy, Minh, Wong, von Haeseler, & Jermiin, 2017) to select appropriate partitions and substitution models before conducting 10 independent IQ-TREE runs of an initial tree search and 10,000 ultrafast bootstrap replicates (BS) for nodal support (Hoang, Chernomor, von Haeseler, Quang Minh, & Sy Vinh, 2018). Partitions and substitution models available for use in MrBayes were determined by PartitionFinder v 2.1.1 (Lanfear, Frandsen, Wright, Senfeld, & Calcott, 2016) using BIC. MrBayes analyses executed 2 runs of 4 chains each for 10^7 MCMC generations sampling every 1,000 trees. Log likelihood scores for each sampling point were analysed using Tracer v 1.7.1 (Rambaut, Drummond, Xie, Baele, & Suchard, 2018) to determine an appropriate burn-in value. Chains were considered stationary when the log likelihood values reached a plateau. Convergence of the two independent runs was monitored using the Potential Scale Reduction Factor (PSRF) of each parameter and the average standard deviation of split frequencies. Strongly supported nodes were represented by BS and PP values greater than 95.

To test for significant differences between BI and ML reconstructions, we implemented an Approximately Unbiased (AU) Test (Shimodaira, 2002) in IQ-TREE using 10,000 RELL replicates (Kishino, Miyata, & Hasegawa, 1990). We chose to implement an AU test in IQ-TREE rather than CONSEL (Shimodaira & Hasegawa, 2001) as it is more appropriate for partitioned analyses considering CONSEL is not partition-aware. Considering trees generated with IQ-TREE and MrBayes are not directly comparable as they were inferred with different models, Mesquite was used to move branches in the ML phylogenetic construction to match the topology resolved by MrBayes for the AU

test. A significance level of $\alpha = 0.05$ was assumed when assessing the statistical significance between topologies.

Genetic diversity and phylogeographic analyses

To get estimates of genetic diversity, we used DnaSP v 6.12.0 (Rozas et al., 2017) to estimate unique haplotypes (h), haplotype diversity (Hd), mean number of nucleotide differences (k) and mean nucleotide diversity (π) at CO1 and ND1 independently for five groups in the *P. ohiensis* species complex: *P. ohiensis*, *P. streckersoni* sp. nov., and three geographic groupings for *P. amphichaenus* (Sabine, Neches, and Trinity drainages). DNA sequence divergence was calculated within and between groups using uncorrected pairwise genetic distances in MEGA7 (Kumar, Stecher, & Tamura, 2016) for CO1 and ND1 independently. Model-based distances have been shown to inflate genetic distance values (Collins & Cruickshank, 2013; Lefébure, Douady, Gouy, & Gibert, 2006; Ratnasingham & Hebert, 2013); therefore, we chose to use uncorrected p-distances to remove biases from nucleotide substitution model assumptions. Partial deletion was used to handle missing data in MEGA7 calculations. To further compare genetic divergence between *P. amphichaenus* and *P. streckersoni* sp. nov., we created histograms of intraspecific and interspecific distance values in the R package ggplot2 (Wickham, 2016). To visualize genetic structuring with respect to geographic distribution, we generated TCS haplotype networks (Clement, Posada, & Crandall, 2000) from CO1 and ND1 independently using PopART 1.7 (Leigh & Bryant, 2015) for groups in the *P. ohiensis* species complex. Missing data were handled using complete deletion, as PopArt does not support partial deletion.

Species delimitation analyses

We implemented the coalescent species delimitation models STACEY v 1.2.4 (Jones, 2017) and *BEAST2 (Ogilvie, Bouckaert, & Drummond, 2017) in BEAST v 2.4.8 (Bouckaert et al., 2014) on a concatenated alignment of CO1 and ND1 for all individuals representing *P. amphichaenus*, *P. ohiensis*, and *P. streckersoni* sp. nov. Partitions and substitutions models for the STACEY analysis were re-evaluated using PartitionFinder (Lanfear et al., 2016) similar to phylogenetic analyses, except allowing for all possible nucleotide evolution models. STACEY infers species boundaries without *a priori* species designations; therefore, we allowed the model to consider all individuals as minimum clusters and freely assign individuals to appropriate clusters. A strict molecular clock was set at 1.0 for the 1st position of CO1 and remaining partitions were estimated by STACEY. Our STACEY analyses consisted of 8 independent runs executing 10^8 generations and logged every 5,000 trees with an initial 10% burn-in. We used LogCombiner v 2.4.8 (Bouckaert et al., 2014) to combine trace logs and species trees from individual runs. We used Tracer to evaluate the combined trace log to ensure convergence of all parameters (ESS $>$ 200). The most likely number of species clusters was calculated by SpeciesDelimitationAnalyser (SpeciesDA) v 1.8.0 (Jones, 2017) using the combined species trees from the 8 individual STACEY runs (144,000 trees). SpeciesDA implemented a collapse height of 0.0001 and a 1.0 simcutoff.

For *BEAST2 analyses, we allowed the most likely species clusters recovered by STACEY to guide our species models. Three species models were implemented to test the log likelihood of clustering scenarios: 1 – *P. amphichaenus* from the Sabine and Neches rivers, *P. amphichaenus* from the Trinity River, *P. ohiensis*, and *P. streckersoni* sp. nov.; 2 – *P. amphichaenus*, *P. ohiensis*, and *P. streckersoni* sp. nov.; and 3 – *P. amphichaenus* from the Sabine and Trinity rivers, *P. amphichaenus* from the Neches River, *P. ohiensis*, and *P. streckersoni* sp. nov. We used the partitions and substitution models appropriate for the STACEY analysis in *BEAST2 analyses, except the substitution model for ND1 1st codon position (K81/TPM1 not available for *BEAST2) which was re-evaluated. *BEAST2 analyses executed 1.5×10^7 generations logging every 5,000 trees to reconstruct a species tree for each scenario. As in the STACEY analyses, a strict molecular clock was set at 1.0 for the 1st position of CO1 and remaining partitions were estimated by *BEAST2. The population model was set to linear with a constant root and the Yule model was the species tree prior. The marginal likelihood of each model was estimated using a path sampling executing 100 path steps with a chain length of 1.5×10^6 and a 25% burn-in (Baele, Li, Drummond, Suchard, & Lemey, 2012; Lartillot & Philippe, 2006). Bayes factors delimitation (BFD) was used to reject species models, using twice the difference of -*ln* likelihood (2*ln*BF) and 2*ln*BF $>$ 10 depicting significant support (Grummer, Bryson, & Reeder, 2014; Kass & Raftery, 1995).

Morphometrics analyses

Traditional and Fourier shape morphometrics were used to compare shell shapes within members of the *P. ohiensis* species complex. Specimens were binned into three groups: *P. amphichaenus* (Sabine, Neches, Trinity; $n = 24$), *P. ohiensis* (Mississippi; $n = 7$), and

P. streckersoni sp. nov. (Brazos; $n = 40$; Table S2, see supplemental material online); specimens showing obvious damage to shells were excluded. For traditional morphometrics, we took four shell measurements: maximum length (anterior to posterior), height 1 (posterior dorsal wing to ventral), height 2 (umbo to ventral), and maximum width (right to left valve) to the nearest 0.01 mm for all specimens using digital callipers (Fig. S1, see supplemental material online). To characterize shell shape, we calculated six ratios: height 1/length (elongation), height 2/length (elongation), height 2/height 1 (wing height), weight/length (inflation), width/height 1 (inflation), and width/height 2 (inflation). Ratios were normalized using an arcsine-transformation. For Fourier shape morphometrics, we used the right valve of each specimen and took digital photographs with a Canon EOS7D SLR camera. The outline of the shell was extracted for each photo by cropping the image using Adobe Photoshop CC v2015.0.0 (Adobe System) (Fig. S1, see supplemental material online). Using the cropped shell image, the shell outline was described by 20 Fourier coefficients using SHAPE v 1.3 (Iwata & Ukai, 2002).

Morphological variation within and among putative species was described through a principal component analysis (PCA) and canonical variate analysis (CVA). Additionally, multivariate analysis of variance (MANOVA) and discriminant function analysis (DFA) were used to determined how frequently principal component (PC) scores correctly distinguished between groups. Confusion matrices were calculated based on the DFA for each morphometric analysis, where percentages of correct group assignments were calculated. Statistical analyses were performed using the software PAST (Hammer, Harper, & Ryan, 2001) and SHAPE. A significance level of $\alpha = 0.05$ was assumed when assessing the statistical significance of all tested hypotheses.

Range map

We compiled distribution data for freshwater mussel surveys conducted in the Brazos River basin to provide information critical for the conservation status assessment of *P. streckersoni* sp. nov. Sources of the distribution data were as follows: Baylor University Mayborn Museum, Fort Worth Museum of Science and History, Texas Parks and Wildlife Department, Joseph Britton Freshwater Mollusk Collection, Texas A&M Natural Resources Institute, Texas Department of Transportation, University of Florida Museum of Natural History, University of Michigan Museum of Zoology, and U.S. Fish and Wildlife Service. We assumed all historical records of *P. ohiensis* and specimens misidentified as *P. amphichaenus* from the Brazos River were *P. streckersoni* sp. nov. We used these distribution data (Table S3, see supplemental material online) to develop a conservation status assessment map using ArcMap 10.3 (ESRI) following the protocol produced by Georgia Department of Natural Resources (2018) and modified approach of Johnson et al. (2016). The spatiotemporal distribution of *P. streckersoni* sp. nov. was illustrated at the Hydrological Unit Code (HUC) 10-level and all known survey locations were included to illustrate both the presence or absence of *P. streckersoni* sp. nov. from 1900–2018.

Results

Taxon sampling

Our molecular matrix consisted of 3204 nucleotides (nt) with each taxon represented by four loci: CO1 (avg. ≈651 nt), ND1 (avg. ≈ 868 nt), ITS1 (647 nt including an avg. of ≈ 23.2% gaps), and 28S (999 nt including an avg. of ≈ 3.6% gaps). All novel DNA sequences were made available on GenBank (MK036068–MK036232; MK044901–MK045202) and Sciencebase (https://doi.org/10.5066/P92CV9QZ), and all accession numbers used in this study can be found in Table S1 (see supplemental material online). We included representatives of all genera in Lampsilini except for *Dromus* Simpson, 1900, which has been shown in previous phylogenetic studies to be closely related to the genus *Cyprogenia* Agassiz, 1852 (Campbell et al., 2005; Zanatta & Murphy, 2006) (Table S1, see supplemental material online). All genera were represented by the type species except *Obovaria* Rafinesque, 1819. All currently recognized species in *Ellipsaria* Rafinesque, 1820, *Leptodea*, *Potamilus*, and *Truncilla* Rafinesque, 1819, were represented in phylogenetic analyses (Williams et al., 2017). In addition to our data matrix for phylogenetic reconstructions, we sequenced a total of 78 individuals from the *P. ohiensis* species complex for CO1 and ND1: *P. amphichaenus* ($n = 29$), *P. ohiensis* ($n = 19$), *P. streckersoni* sp. nov. ($n = 30$; Fig. 1; Table S1, see supplemental material online). Both CO1 and ND1 alignments did not contain indels or stop codons.

Phylogenetic reconstruction

Xia's saturation test indicated little saturation at all codon positions for CO1 and ND1; therefore, all codon positions were retained in phylogenetic analyses. Nucleotide substitution models were determined for eight partitions by ModelFinder for IQ-TREE analyses: CO1 1st position – TN + F + I + G4, CO1 2nd position

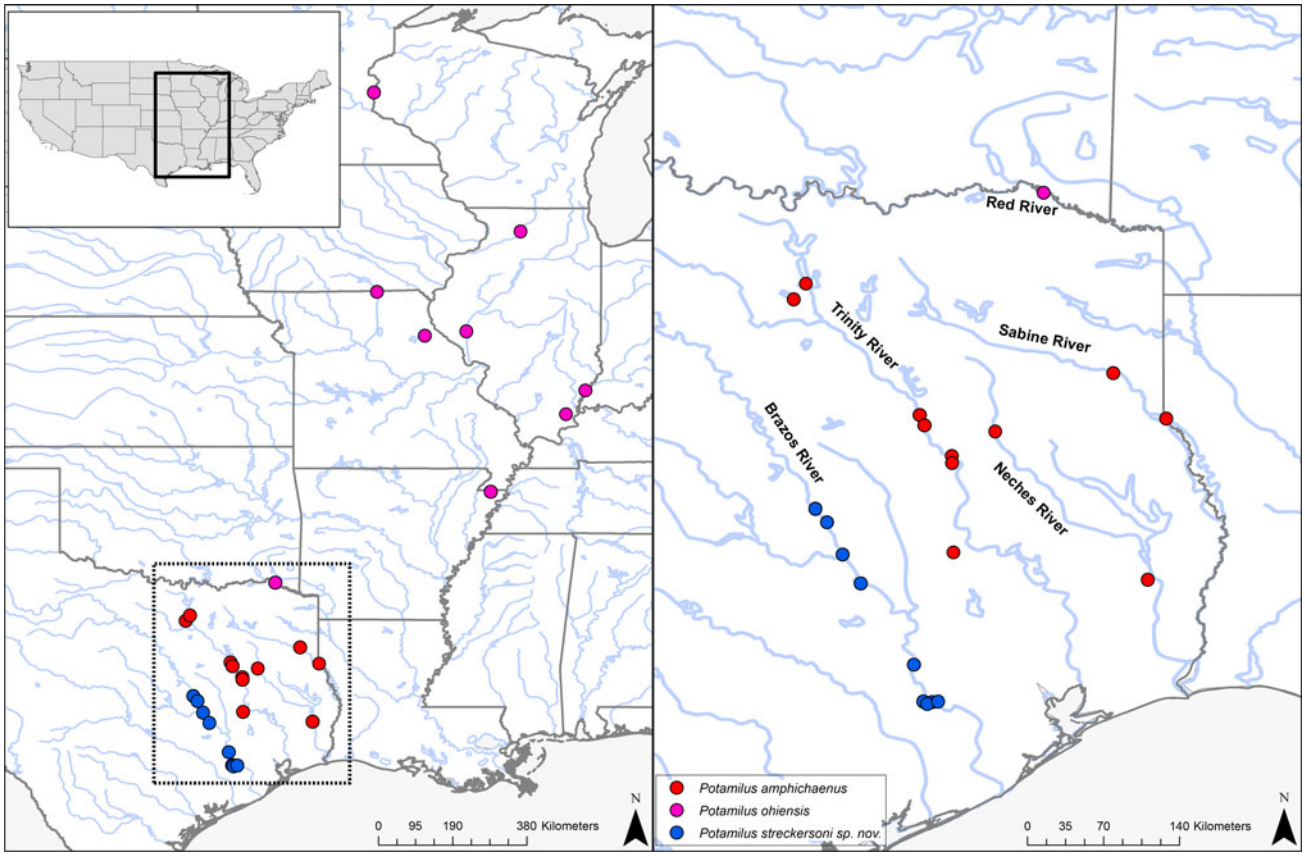

Fig. 1. Collection localities for specimens in the *Potamilus ohiensis* species complex used in this study. Colours correspond to the species in the complex: *P. amphichaenus* (Sabine, Neches, and Trinity River drainages), *P. ohiensis* (Mississippi River drainage), and *P. streckersoni* **s**p. nov. (Brazos River drainage).

– TPM3 + F, CO1 3rd position – TVM + F+G4; ND1 1st position – TIM2e + I+G4, ND1 2nd position – TIM2 + F + I + G4, ND1 3rd position – TIM + F+G4, ITS1- TIM2e + I+G4, and 28S – TN + F + I + G4. For BI analyses, nucleotide substitution models were determined for seven partitions by PartitionFinder: CO1 1st position and ND1 2nd position – HKY + I + G, CO1 2nd position – F81 + I, CO1 3rd position – GTR + G, ND1 1st position – SYM + I + G, ND1 3rd position – GTR + G. ITS1- K80 + I + G, and 28S – HKY + I + G. Convergence of the two MrBayes runs was supported by the PSRF value for each parameter equal to 1.0 and the mean of the standard deviation of split frequencies (0.001288). A 25% burnin was deemed appropriate for each MrBayes run by Tracer and was implemented before optimal log likelihood and trees were reported.

Both ML and BI topologies resolve a monophyletic grouping of *Ellipsaria*, *Leptodea*, *Potamilus*, and *Truncilla* (Figs 2, S2, see supplemental material online); however, supraspecific relationships between these genera were not resolved with strong nodal support. Topologies depict four strongly supported clades (PP/BS = 100): *Ellipsaria* and *Truncilla*; *L. fragilis* and *L. leptodon*; *P. amphichaenus*, *P. ohiensis*, and *P. streckersoni* sp. nov.; and *P. alatus*, *P. metnecktayi*, and *P. purpuratus*. Topologies strongly support *P. streckersoni* sp. nov. sister to *P. amphichaenus* rather than *P. ohiensis*, with significant divergence from both species. Phylogenetic placement of *L. ochracea*, *P. capax*, and *P. inflatus* were inconsistent between ML and BI analyses (Figs 2, S2, see supplemental material online). To test these inconsistencies, we implemented an AU test but no significant difference between BI and ML topologies was recovered ($\alpha = 0.5018$).

Phylogeographic analyses

Genetic diversity statistics generated by DnaSP are reported in Table 1 for members of the *P. ohiensis* species complex. High levels of genetic diversity were depicted in *P. ohiensis* and the Trinity River population of *P. amphichaenus*, while *P. streckersoni* sp. nov. depicted excessive haplotype sharing and limited nucleotide diversity. Mean pairwise genetic distance values for within and between groups at CO1 and ND1 are reported in Table 2. Distance values for CO1 and ND1

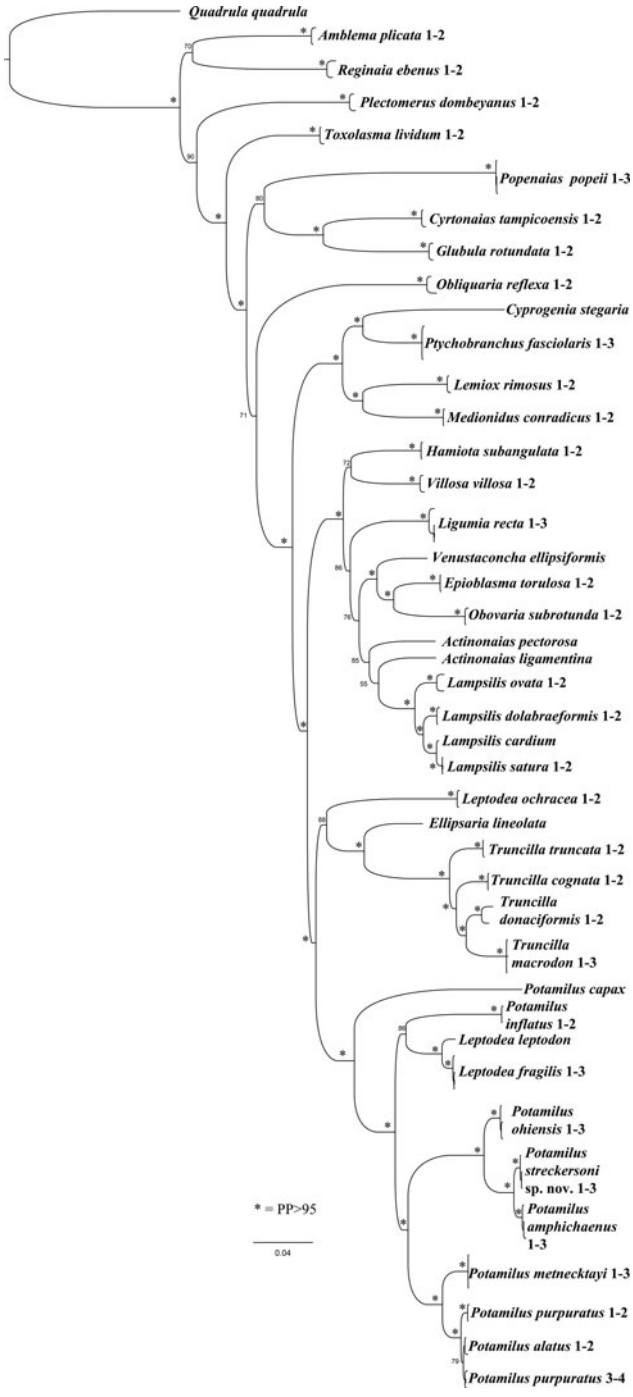

Fig. 2. Bayesian inference topology reconstructed using MrBayes on a concatenated molecular matrix (CO1, ND1, ITS1, 28S). Values above branches represent posterior probabilities (PP). Strongly supported nodes (i.e., PP $\geq$ 95) are indicated by asterisks.

depicted *P. ohiensis* largely divergent from both *P. amphichaenus* and *P. streckersoni* sp. nov. (Table 2). Genetic distance between *P. streckersoni* sp. nov. and all populations of *P. amphichaenus* at CO1 and ND1 ranged from 1.81–2.29% and 1.59–2.15%, respectively (Table 2). Histograms of intra- and interspecific uncorrected p-distance values for *P. amphichaenus* and *P. streckersoni* sp. nov. depicted clear separation between intraspecific variation and interspecific divergence (Figs S3.1 & S3.2, see supplemental material online). TCS haplotype networks also showed clear divergence at mtDNA markers between *P. amphichaenus*, *P. ohiensis*, and *P. streckersoni* sp. nov. and depicted limited divergence within *P. amphichaenus* with respect to drainage of capture at ND1 (Fig. 3.2). Similar to genetic diversity statistics, haplotype networks depicted excessive haplotype sharing in *P. streckersoni* sp. nov. at both mtDNA markers.

Species delimitation analyses

The molecular matrix used in the STACEY and *BEAST2 analyses was aligned to 1558 bp and included all individuals in the *P. ohiensis* species complex. Five partitions and substitution models were selected for STACEY and *BEAST2 by PartitionFinder: CO1 1st position – HKY, CO1 and ND1 2nd position – HKY, CO1 3rd position – HKY, ND1 1st position – TPM1, and ND1 3rd position – TrN. TPM1 is not available in *BEAST2; therefore, we implemented K80, the most-appropriate substitution model available for the analysis. Convergence of the STACEY and *BEAST2 analyses was indicated by all ESS values $>$ 200. STACEY resolved three species models with probabilities greater than 5%, but not with high probabilities: Species Model 1 (27.2%) – *P. amphichaenus* from the Sabine and Neches drainages, *P. amphichaenus* from the Trinity drainage, *P. ohiensis*, and *P. streckersoni* sp. nov.; Species Model 2 (21.2%) – *P. amphichaenus*, *P. ohiensis*, and *P. streckersoni* sp. nov.; and Species Model 3 (12.5%) – *P. amphichaenus* from the Sabine and Trinity drainages, *P. amphichaenus* from the Neches drainage, *P. ohiensis*, and *P. streckersoni* sp. nov. (Fig. 4; Table 3). *BEAST2 analyses resolved Species Model 1 as the most likely, and 2*ln*BF rejected Species Model 2 but could not reject Species Model 3 (Table 3).

Morphometric analyses

For traditional morphometrics, the PCA yielded three distinct eigenvalues that described $>$ 99% of the total variation among individuals, with the first two PCs describing 90.69% of the total variation (Fig. 5). The PCA and CVA plots showed differentiation among species, where a small portion of the cluster of *P. amphichaenus* overlapped with the cluster of *P. streckersoni* sp. nov. (Figs 5.1 & 5.2). The MANOVA depicted that

Table 1. Summary statistics for genetic diversity within *Potamilus amphichaenus*, *Potamilus ohiensis*, and *Potamilus streckersoni* sp. nov., including number of unique haplotypes (h), haplotype diversity (Hd), average number of nucleotide differences (k), and nucleotide diversity (π) for CO1 and ND1.

Taxa (Drainage; Sample Size)	CO1				ND1			
	h	Hd	k	π	h	Hd	k	π
***P. amphichaenus* (Sabine; *n* = 2)**	1	0	0	0	1	0	0	0
***P. amphichaenus* (Neches; *n* = 4)**	1	0	0	0	1	0	0	0
***P. amphichaenus* (Trinity; *n* = 23)**	3	0.17	0.17391	0.00027	8	0.715	0.97233	0.00110
***P. ohiensis* (Mississippi; *n* = 19)**	5	0.591	0.86550	0.00166	5	0.462	0.70175	0.00084
***P. streckersoni* sp. nov. (Brazos; *n* = 30)**	2	0.239	0.23908	0.00043	2	0.067	0.06667	0.00008

Table 2. Mean intra- and interspecific genetic uncorrected p-distance values for *Potamilus amphichaenus*, *Potamilus ohiensis*, and *Potamilus streckersoni* sp. nov. CO1 values are represented in the lower triangle and ND1 in the upper triangle.

Taxa (Drainage; Sample Size)	1	2	3	4	5	Within Group CO1	Within Group ND1
1. *P. amphichaenus* (Sabine; *n* = 2)		0.11 (N/A)	0.50 (0.44-0.67)	7.33 (7.09-7.52)	1.88 (1.78-1.91)	0	0
2. *P. amphichaenus* (Neches; *n* = 4)	0.16 (0.15-0.16)		0.40 (0.33-0.57)	7.17 (6.83-7.40)	1.74 (1.59-1.79)	0	0
3. *P. amphichaenus* (Trinity; *n* = 23)	0.02 (0-0.16)	0.17 (0.15-0.32)		7.12 (6.78-7.52)	1.93 (1.69-2.15)	0.03 (0-0.30)	0.11 (0-0.34)
4. *P. ohiensis* (Mississippi; *n* = 19)	5.08 (4.83-5.33)	4.87 (4.65-5.07)	5.04 (4.83-5.37)		7.34 (6.84-7.52)	0.13 (0-0.61)	0.09 (0-0.48)
5. *P. streckersoni* sp. nov. (Brazos; *n* = 30)	2.03 (1.98-2.18)	1.87 (1.81-2.06)	2.02 (1.98-2.29)	4.10 (3.81-4.41)		0.04 (0-0.18)	0.01 (0-0.12)

shell morphologies were significantly different among species (Wilk's $\Lambda = 0.1298$; $F_{12,126} = 18.65$; $p < 0.001$; Table 4). On average, the DFA assigned 85.9% of individuals to the correct group (Table 4).

For Fourier shape morphometrics, the PCA yielded six distinct eigenvalues and described >90% of the total variation among individuals (Fig. 5). The PCA and CVA plots showed similar clustering patterns to the traditional morphometrics (Figs 5.3 & 5.4), with divergence between species and limited overlap between *P. amphichaenus* and *P. streckersoni* sp. nov. The MANOVA depicted significant differences in shell morphologies between species (Wilk's $\Lambda = 0.1756$; $F_{12,126} = 14.56$; $p < 0.001$; Table 4). Fourier morphometrics had a slightly better assignment rate, with 90.1% of individuals assigned to the correct group (Table 4).

Range map. During our searches of museum records and available field observations, we located collection information for 2,049 freshwater mussel surveys conducted from 1900–2018 in the Brazos River basin. Shells (fresh dead or recently dead) or live individuals of *P. streckersoni* sp. nov. were reported during 213 surveys conducted from 1934–2018 (Table S3, see supplemental material online), including a total of 231 live individuals. *Potamilus streckersoni* sp. nov. records were distributed across 27 HUC units in the Brazos River basin (Fig. 6). The status of the species in each HUC unit was categorized as follows: 13 HUCs with shell only; 3 with historical records (prior to 1995); 2 with recent records (1995–2010); and 9 with current records (2011 to present).

Taxonomic accounts

Potamilus streckersoni sp. nov.
Brazos Heelsplitter

Holotype: UF439497, length 128 mm, Brazos River upstream of FM 485 bridge (30.86586°N, −96.69575°W), Milam/Robertson Counties, TX, 10 Nov. 2017 (Fig. 7).

Paratypes: UF439478, 4 wet specimens, length 93–117 mm, Brazos River upstream of FM 485 bridge (30.86586°N, −96.69575°W), Milam/Robertson Counties, TX, 10 Nov. 2017.

UF441294, 4 wet specimens, length 76–105 mm, Brazos River about 1 mile downstream of FM1093, about 2.7 miles ENE of Wallis, TX (29.650845°N, −96.026521°W), Austin/Fort Bend Counties, TX, 24 Oct. 2012.

Etymology: The specific epithet *streckersoni* is in honour of John K. Strecker and Lorraine L. Frierson. John K. Strecker, former curator of the Baylor University Museum (Waco, TX, USA), authored one of the first

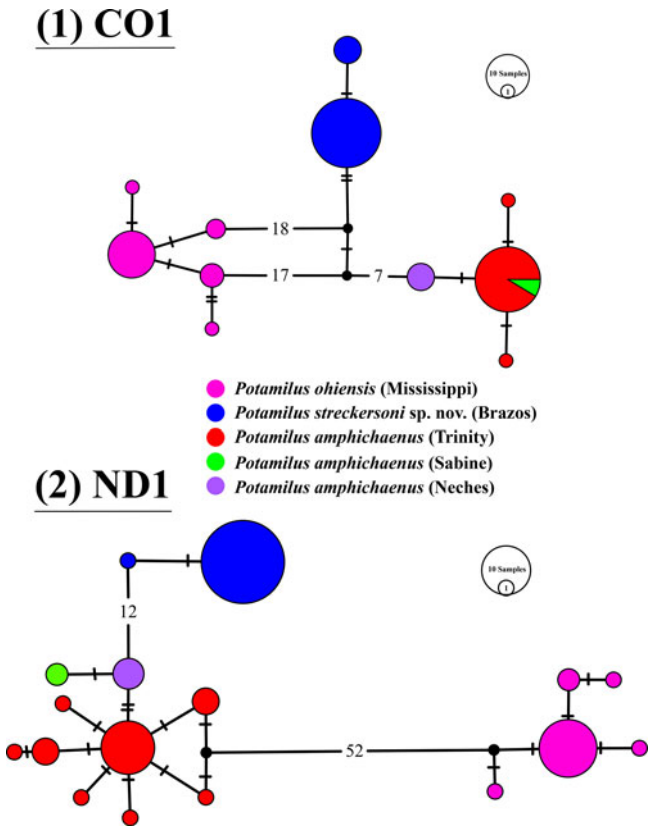

Fig. 3. Haplotype networks based on CO1 (3.1) and ND1 (3.2) from individuals in the *Potamilus ohiensis* species complex. Each circle represents a unique haplotype with size relative to the number of individuals with each haplotype. Black circles represent unsampled haplotypes and individual tick marks or numbers indicate nucleotide substitutions between haplotypes.

publications regarding distribution and biodiversity of Texas unionids (Strecker, 1931), which provided the foundation for freshwater mussel conservation in Texas. He had a strong relationship with esteemed malacologist Mr Lorraine L. Frierson, who corresponded nearly 20 years with Mr Strecker regarding mussel taxonomy and identification. Between Strecker and Frierson, 2,277 unionid specimens were collected and donated to the Mayborn Museum at Baylor University.

Diagnosis: *Potamilus streckersoni* sp. nov. is significantly different from *P. ohiensis* using both molecular and morphological characters (Figs 3, 4 & 5; Tables 2 & 4). Of the 30 *P. streckersoni* sp. nov. and 19 *P. ohiensis* individuals we examined, the two taxa were diagnosable at 25 of 658 sites examined at CO1 and 66 of 900 sites examined at ND1. *Potamilus streckersoni* sp. nov. is also morphologically divergent, with individuals more elongate and less alate than specimens of *P. ohiensis* (Fig. 5; Table 4); however, future work evaluating additional material from throughout the range of *P. ohiensis* is encouraged to better assess the wide range of morphological variation in this species.

Potamilus streckersoni sp. nov. can be diagnosed from other similar sympatric freshwater mussels in the Brazos River using conchological characters including periostracum colour, lack of sculpturing, reduced umbo, and absence or weak posterior ridge. *Potamilus streckersoni* sp. nov. may be confused with *Cyrtonaias tampicoensis* (Lea, 1838) or *P. purpuratus*; however, *P. streckersoni* sp. nov. is generally more elongate than both species. The pseudocardinal teeth of *P. streckersoni* sp. nov. are less developed and only one tooth is present in the left valve, while *C. tampicoensis* and *P. purpuratus* have two well-developed pseudocardinal teeth in the left valve. *Potamilus streckersoni* sp. nov. may also be confused with *L. fragilis*. Larger specimens of *P. streckersoni* sp. nov. are typically less elongate than similar sized *L. fragilis*, and the dark brown periostracum is easily distinguishable from the horn yellow periostracum of *L. fragilis*. In smaller individuals where periostracum colour may not be diagnostic, *P. streckersoni* sp. nov. can be distinguished from *L. fragilis* by presence of an anterior dorsal wing, which is absent in *L. fragilis*.

Description: Maximum shell length to 144 mm (JBFMC26.1). Shell thin to moderately thick and

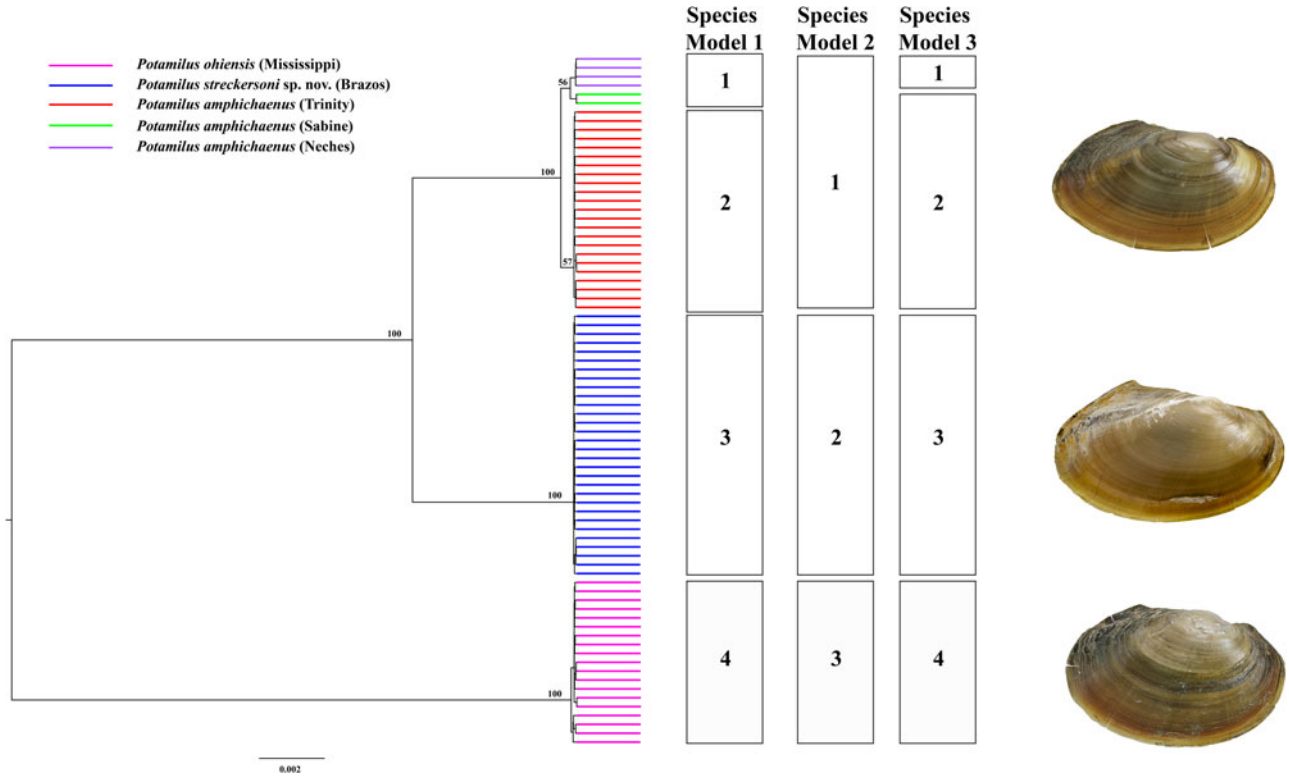

Fig. 4. Inference from coalescent-based species delimitation models. The phylogeny represents the topology resolved by STACEY with posterior probabilities (PP) presented above nodes for each clade of interest. Each line represents an individual sampled and colours correspond to species and drainage of capture. Species models implemented in *BEAST2 are shown to the right, along with photographs of *Potamilus amphichaenus*, *Potamilus ohiensis*, and *Potamilus streckersoni* sp. nov.

Table 3. Species models implemented in *BEAST2 following results from most likely species clusters in STACEY analyses. Values in bold font represent Bayes factors that are significantly worse than the best model.

Species Model	STACEY Probability	*BEAST2 *ln*	2*ln*BF	Reject
1	27.2%	−2898.01	–	–
2	21.2%	−2915.19	**34.37**	**Yes**
3	12.5%	−2899.09	2.17	No

compressed. General outline of the shell is oval; however, may be triangular in smaller individuals when posterior dorsal wing has not been eroded or broken; posterior and anterior margins rounded. Dorsal margin with weak wing posterior to umbo, which is typically more prominent in smaller individuals. Small triangular dorsal wing anterior to umbo in smaller specimens, usually eroded away in larger individuals. Ventral margin straight to convex, posterior ridge absent or very low, posterior slope flattened to slightly concave, merging with the posterior dorsal wing. Umbo low, broad, and barely extends above the hinge line, with limited sculpturing. Periostracum shiny, greenish to yellowish in smaller specimens, becoming chestnut brown in larger individuals. Pseudocardinal teeth compressed and delicate, one in each valve with an accessory denticle usually present in right valve. Lateral teeth moderately long, slightly curved, two in left valve and one in right. Interdentum moderately long, narrow; umbo cavity wide but shallow. Nacre deep pink or purple.

Distribution: *Potamilus streckersoni* sp. nov. is endemic to the Brazos River drainage in Texas. Historical records indicate *P. streckersoni* sp. nov. occurred throughout the mainstem Brazos River and most of its tributaries. Recent survey efforts, however, depict that it is likely extirpated from much of its historical range (Fig. 6). Two isolated populations may still be extant north of current impoundments coinciding with river segments between Lake Granbury and Lake Whitney, and north of Possum Kingdom Reservoir.

Remarks: The systematic placement of *P. streckersoni* sp. nov. suggests this species is a host fish specialist,

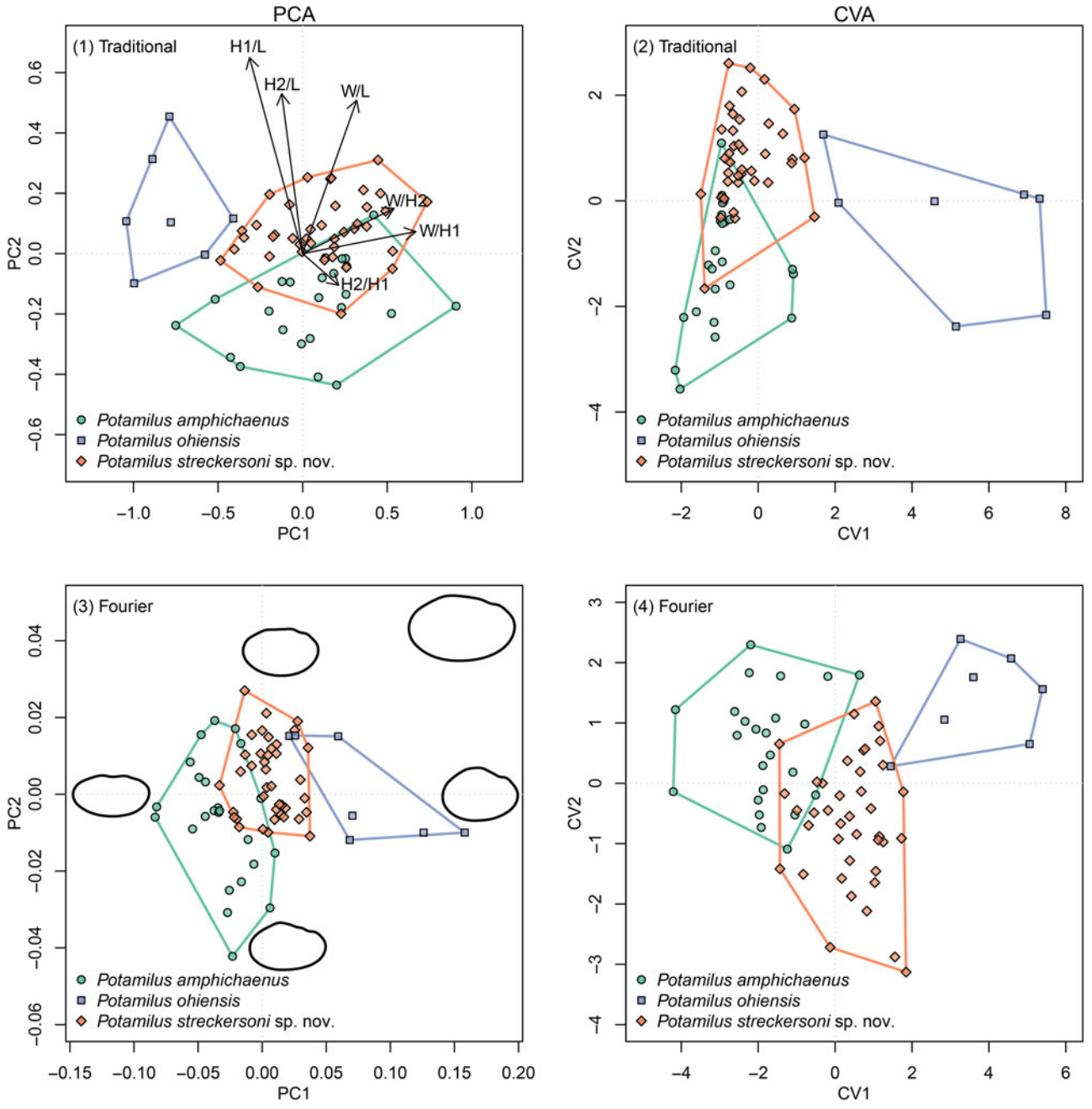

Fig. 5. Scatter plots from principal component analysis (PCA) and canonical variate analysis (CVA) of traditional (5.1, 5.2) and Fourier (5.3, 5.4) morphometrics. Colours and shapes of points correspond to putative species (green = *Potamilus amphichaenus*, blue = *Potamilus ohiensis*, orange = *Potamilus streckersoni* sp. nov.). Polygons enclose convex hulls of each species. Biplots of variables from traditional morphometrics (5.1) are shown in arrows. Outlined shell shapes from Fourier morphometrics (5.3) represent a mean shape (top-right) and ±2 × SD on PC1 and PC2 axes.

with glochidia that complete metamorphosis on *A. grunniens*. Additionally, *Potamilus streckersoni* sp. nov. is likely a long-term brooder and gravid females have been collected in May (UF439481), October (UF441294), and November (UF439478). Future research focused on characterizing host fish use and brooding characteristics is needed to confirm these hypotheses.

Dams and other features in the Brazos River basin likely limit dispersal of *P. streckersoni* sp. nov. and some populations may represent evolutionarily significant units (ESUs) or management units (MUs) (see

Table 4. Significance values (p) for pairwise comparisons of morphometric analyses with traditional morphometric values represented in the lower triangle and Fourier shape morphometrics represented in the upper triangle, along with the percentage of individuals binned accurately by discriminant function analyses (DFA) for traditional and Fourier shape morphometrics.

Taxa	1	2	3	Traditional DFA	Fourier DFA
1. P. amphichaenus		2.08E-08	1.71E-09	83.3%	87.5%
2. P. ohiensis	4.73E-09		9.15E-08	71%	85.7%
***3. P. streckersoni* sp. nov.**	3.00E-07	4.29E-12		90.0%	92.5%

Moritz 1994). Additional mussel surveys coupled with an evaluation of population genetic structure using fine-scale genomic markers (e.g., microsatellites, GBS, etc.) would be essential for delineating populations as ESUs or MUs and may help direct future conservation and management efforts.

Discussion

Supraspecific relationships in Lampsilini

Our data supports that evolutionary relationships in Lampsilini have largely been shaped by life history characters, as we see a strong correlation between host fish use, host infection strategies, and phylogenetic placement. More specifically, our analyses resolved a monophyletic group consisting of *Ellipsaria*, *Leptodea*, *Potamilus*, and *Truncilla*. In general, these four genera are linked by two synapomorphic characters unique to Lampsilini: being host specialists, with glochidia only transforming on freshwater drum, *Aplodinotus grunniens* Rafinesque, 1819; and the growth of glochidia during encapsulation (i.e., while attached to host) (Barnhart et al., 2008; Roe, Simons, & Hartfield, 1997; Sietman et al., 2018; Williams et al., 2008). Despite strong behavioural and morphological characters supporting the monophyly of this group, BI and ML reconstructions depict incongruence regarding relationships between species in these genera, primarily regarding the placement of species in *Leptodea* and *Potamilus* (Figs 2 & S2, see supplemental material online). More specifically, the phylogenetic placement of *L. ochracea*, *P. capax*, and *P. inflatus* is incongruent between the BI and ML phylogenies. The generic placement of *L. ochracea* has been questioned due to significant morphological divergence from remaining species of *Leptodea* (Davis & Fuller, 1981; Johnson, 1970; Smith, 2000; Stiven & Alderman, 1992). Furthermore, the use of *A. grunniens* as a host is not possible considering their ranges do not overlap (Johnson, 1970; Page & Burr, 2011). In the BI topology, *L. ochracea* was resolved sister to *Ellipsaria* and *Truncilla* with relatively low posterior support, while ML resolved *L. ochracea* sister to *Potamilus* and the remaining species in *Leptodea*. We see similar patterns of incongruence in *Potamilus*, with *P. inflatus* resolved basal to a monophyletic clade of *L. fragilis*, *L. leptodon*, and remaining members of *Potamilus*, while *P. capax* is resolved sister to a monophyletic clade comprised of *L. fragilis* and *L. leptodon* in our ML reconstruction. However, the position of two species switch in BI topologies with *P. capax* resolved basal and *P. inflatus* resolved sister to *L. fragilis* and *L. leptodon*. To test these incongruences, we implemented an AU test and results indicated no significant differences between BI and ML reconstructions ($p = 0.4831$), likely due to weak nodal support (i.e., BS/PP) for phylogenetic relationships between *Leptodea* and *Potamilus* species.

Our study represents the first robust phylogenetic evaluation of *Leptodea* and *Potamilus* with comprehensive taxon sampling and evaluation of both mtDNA and nDNA loci. Despite employing multiple independently evolving markers used in recent freshwater mussel phylogenetic studies (Johnson et al., 2018; Lopes-Lima et al., 2017; Perkins et al., 2017; Pfeiffer, Sharpe, Johnson, Emery, & Page, 2018; Pfeiffer et al., 2016; Pieri et al., 2018; Smith et al., 2018), we could not resolve topologies that strongly support phylogenetic relationships between *Leptodea* and *Potamilus*. Therefore, we take a precautionary approach by not making any conclusions regarding generic-level assignments at this time. However, our evaluation and comprehensive taxon sampling provides a baseline for future hypotheses regarding phylogenetic relationships of lampsiline genera. We believe that future investigations focusing on glochidial morphology and next-generation sequencing technologies targeting conserved but phylogenetically informative loci (Faircloth et al., 2012; Lemmon, Emme, & Lemmon, 2012) will be necessary to elucidate supra-specific relationships and move forward with any generic-level taxonomic revisions.

Species boundaries in the *Potamilus ohiensis* species complex

Based on previous taxonomic accounts, *P. ohiensis* is assumed to occur in the Mississippi River drainage with disjunct populations in the Brazos River (Howells et al., 1996). This distributional pattern is thought to be a result of historical stream capture events, as seen in

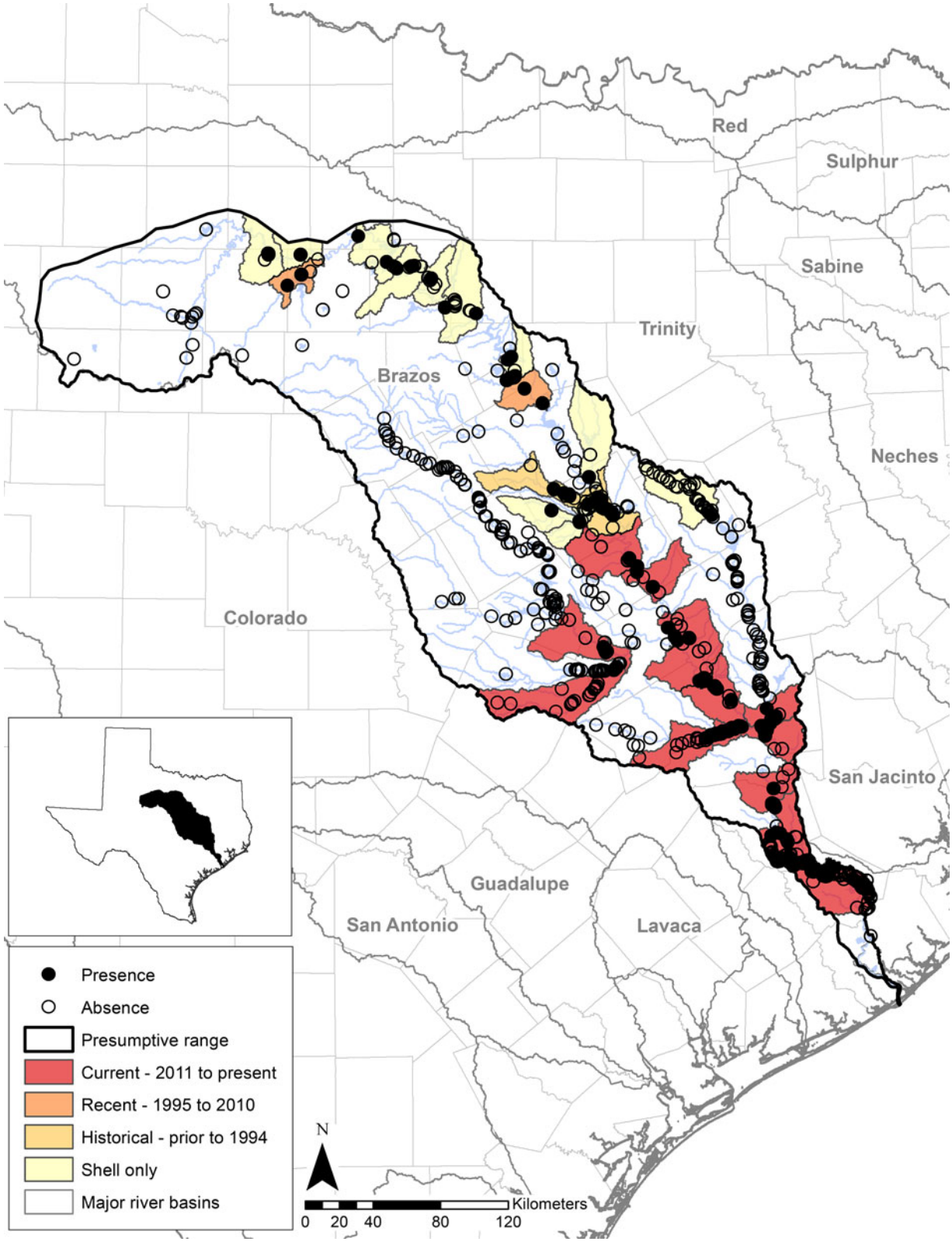

Fig. 6. Conservation status map for *Potamilus streckersoni* sp. nov. (Brazos Heelsplitter). Shaded circles denote presence and unshaded circles indicate absence. Hydrologic Unit Codes (HUC) 10-level are coloured based on live versus shell. For the former, HUCs are further shaded by when a live specimen of *P. streckersoni* sp. nov. was collected. Solid black line denotes the presumptive range.

Fig. 7. *Potamilus streckersoni* sp. nov. holotype (UF439497).

other freshwater fish and mussel species (Haag, Warren, Wright, & Shaffer, 2002; Hubbs, Edwards, & Garrett, 1991; Smith et al., 2018). However, the results of our phylogenetic and phylogeographic analyses resolve *P. streckersoni* sp. nov. closely related to *P. amphichaenus*, rather than a conspecific of *P. ohiensis* from the Interior Basin. Results also depict clear genetic separation between *P. amphichaenus* and *P. streckersoni* sp. nov., and no evidence for the two species existing in sympatry in the Trinity River drainage. These findings are similar to other faunal relationships in the western Gulf of Mexico drainages, given the high levels of endemism across these drainages (Haag & Williams, 2014; Howells et al., 1996; Hubbs, 1957; Hubbs et al., 1991; Strecker, 1931).

Allopatry is known as the driving force in many speciation processes (Mayr, 1942, 1963) and many riverine speciation events are indicative of extended periods of genetic isolation (Jordan, 1905; Mayr, 1959), including diversification of freshwater mussels (Inoue, McQueen, Harris, & Berg, 2014; Johnson et al., 2018; Smith et al., 2018). However, resolving speciation processes from patterns of genetic drift via metapopulation structure continues to confound modern systematic research (De Queiroz, 2007; Leaché, Zhu, Rannala, & Yang, 2019; Sukumaran & Knowles, 2017). In the case of *P. streckersoni* sp. nov., if allopatric population structure was responsible for divergence, we would expect to see similar patterns of divergence between populations of *P. amphichaenus* (i.e., Sabine, Neches, and Trinity drainages). However, we see limited levels of divergence in *P. amphichaenus* populations and haplotype sharing in peripheral populations (Table 2; Figs 3.1 & 3.2). Phylogeographic analyses suggest an extended period of allopatry of *P. streckersoni* sp. nov. from all populations of *P. amphichaenus*. Genetic distances between the two entities are similar to or greater than patterns of species-level diversity in other unionids (Inoue et al., 2014a; Jones, Neves, Ahlstedt, & Hallerman, 2006; Pfeiffer et al., 2016; Pieri et al., 2018; Roe & Lydeard, 1998), and haplotype networks depicting clear molecular separation between *P. streckersoni* sp. nov. and *P. amphichaenus* with no haplotype sharing at either mtDNA markers (Figs 3.1 & 3.2). We also see a clear gap between intra- and interspecific genetic distance (Figs S3.1 & S3.2, see supplemental material online), indicative of a long period of genetic isolation.

To further investigate species boundaries in the *P. ohiensis* species complex, we employed two coalescent-based species delimitation models: STACEY and *BEAST2. STACEY resolved four strongly supported species clusters without *a priori* designation as the most likely species model: *P. amphichaenus* from the Sabine and Neches drainages, *P. amphichaenus* from the Trinity drainage, *P. ohiensis*, and *P. streckersoni* sp. nov. (Fig. 4). However, there was not decisive support based on the probability of the model; therefore, we implemented *BEAST2 to test the marginal likelihood of the three most likely species scenarios identified by STACEY. *BEAST2 analyses depicted significant support for the recognition of four species clusters in the *P. ohiensis* species complex; however, models could not find significant support for a consensus designation of the two clusters recognized within *P. amphichaenus* (Table 3). Species Model 1 recognized *P. amphichaenus* from the Sabine and Neches, and *P. amphichaenus* from the Trinity as distinct species, which reconstructs a similar biogeographic pattern recovered in a recent assessment of species-level diversity in another group of unionids (Pieri et al., 2018). Despite this congruence with a previous study, Species Model 1 was only found marginally better than Species Model 3 (Table 3), which groups peripheral populations of *P. amphichaenus* as a species cluster (Sabine and Trinity). These results are likely due to haplotype sharing and lack of monophyly between the peripheral populations of *P. amphichaenus* (i.e., Sabine and Trinity drainages) at CO1, indicative of limited divergence time and the possibility of on-going gene flow (Fig. 3.1). Furthermore, coalescent-based approaches have been repeatedly criticized for delimiting population structure rather than species (Leaché et al., 2019; Sukumaran & Knowles, 2017), and have been shown to inflate estimates of biodiversity in freshwater mussels (Pfeiffer et al., 2016; Smith et al., 2018). We believe that STACEY and *BEAST analyses overestimate the biodiversity in *P. amphichaenus* and agree with previous research that when used alone, coalescent-based species delimitation models may be insufficient

for taxonomic evaluations (Fujita et al., 2012; Leaché et al., 2019).

Similar to molecular evidence, we see strong morphological divergence between members of the *P. ohiensis* species complex. MANOVAs of traditional and Fourier shape morphometrics depicted significant divergence between *P. amphichaenus*, *P. ohiensis*, and *P. streckersoni* sp. nov. (Table 4). We did observe slight overlap between *P. amphichaenus* and *P. streckersoni* sp. nov. However, DFAs for both traditional and Fourier shape morphometrics were able to assign *P. streckersoni* sp. nov. correctly from other members of *P. ohiensis* species complex 90% and 92.5% of the time, respectively. These values are similar to or higher than studies utilizing similar morphological analyses to resolve species boundaries in freshwater mussels (Gangloff, Williams, & Feminella, 2006; Inoue et al., 2014; Johnson et al., 2018; Pieri et al., 2018), indicative of significant morphological divergence of *P. streckersoni* sp. nov. from *P. amphichaenus*. However, our morphological dataset does have several weaknesses. Morphological characteristics, especially external shell morphology in unionids, can be the result of environmental variables (Eagar, 1950; Ortmann, 1920). Furthermore, our sample sizes are low when compared with other species-delimitation studies incorporating morphological data (Inoue et al., 2014; Johnson et al., 2018; Pieri et al., 2018; Smith et al., 2018); especially for *P. ohiensis*, a wide-ranging species that likely depicts high levels of morphological plasticity throughout its range. Despite this, molecular data clearly depict that *P. ohiensis* is divergent from other members of the species complex; therefore, we focused interpretation of our morphological assessment on species delimitation between *P. amphichaenus* and *P. streckersoni* sp. nov.

Inference from our integrative taxonomic assessment provides significant support for the recognition of a new species, *P. streckersoni* sp. nov. and we see clear separation of three well-supported taxonomic entities in the *P. ohiensis* species complex: *P. amphichaenus*, *P. ohiensis*, and *P. streckersoni* sp. nov. These three lineages exhibit clear divergence at mtDNA markers (Table 2; Figs 3.1 & 3.2), depict significant differences in shell shape (Table 4; Fig. 5), and are geographically diagnosable. Considering the congruence across molecular, morphological, and geographic data, we have formally described *P. streckersoni* sp. nov.

Acknowledgements

The authors wish to thank Caitlin Beaver, Celine Carneiro, and Kaitlyn Havlik for assistance in the laboratory; along with Andy Blair, Tony Brady, Ken Brown, Robert Butler, Kevin Cummings, Chris Davidson, Gerry Dinkins, Matthew Duplessis, Scott Faiman, Mark Fisher, Andy Ford, Jeff Garner, John Harris, Michael Hart, Tyler Hern, Kevin Kocot, Jeff Powell, Sandy Pursifull, Clint Robertson, Daniel Schilling, Charrish Stevens, Rachel Vinsel, Jim Williams, Alabama Museum of Natural History, Florida Museum of Natural History, Illinois Natural History Survey, and McClung Museum of Natural History for assistance with collections. Additional thanks to Manuel Lopes-Lima, Elliot Shubert, Jim Williams, Andrea Waeschenbach, and one anonymous reviewer for comments on the manuscript during the review process and special thanks to Jeff Powell for help obtaining funding, which was provided to Nathan A. Johnson by U.S. Fish and Wildlife Service and U.S. Geological Survey. All molecular, morphometric, and distribution data used in this study are available on Sciencebase (https://doi.org/10.5066/P92CV9QZ). Any use of trade, firm, or product names is for descriptive purposes only and does not imply endorsement by the U. S. Government.

Disclosure statement

No potential conflict of interest was reported by the authors.

Supplemental data

Supplemental data for this article can be accessed here: https://dx.doi.org/10.1080/14772000.2019.1607615.

ORCID

Chase H. Smith http://orcid.org/0000-0002-1499-0311
Nathan A. Johnson http://orcid.org/0000-0001-5167-1988
Kentaro Inoue http://orcid.org/0000-0001-6087-3290
Robert D. Doyle http://orcid.org/0000-0003-2121-0712
Charles R. Randklev http://orcid.org/0000-0002-6755-1507

References

Baele, G., Li, W. L. S., Drummond, A. J., Suchard, M. A., & Lemey, P. (2012). Accurate model selection of relaxed molecular clocks in Bayesian phylogenetics. *Molecular Biology and Evolution*, *30*, 239–243.

Barnhart, M. C., Haag, W. R., & Roston, W. N. (2008). Adaptations to host infection and larval parasitism in

Unionoida. *Journal of the North American Benthological Society*, *27*, 370–394.
Bouckaert, R., Heled, J., Kühnert, D., Vaughan, T., Wu, C.-H., Xie, D., … Drummond, A. J. (2014). BEAST 2: A software platform for Bayesian evolutionary analysis. *Public Library of Science Computational Biology*, *10*, e1003537.
Campbell, D. C., Serb, J. M., Buhay, J. E., Roe, K. J., Minton, R. L., & Lydeard, C. (2005). Phylogeny of North American amblemines (Bivalvia, Unionoida): Prodigious polyphyly proves pervasive across genera. *Invertebrate Biology*, *124*, 131–164.
Chernomor, O., von Haeseler, A., & Minh, B. Q. (2016). Terrace aware data structure for phylogenomic inference from supermatrices. *Systematic Biology*, *65*, 997–1008.
Clement, M., Posada, D., & Crandall, K. A. (2000). TCS: A computer program to estimate gene genealogies. *Molecular Ecology*, *9*, 1657–1659.
Collins, R. A., & Cruickshank, R. H. (2013). The seven deadly sins of DNA barcoding. *Molecular Ecology Resources*, *13*, 969–975.
Davis, G. M., & Fuller, S. L. H. (1981). Genetic relationships among recent Unionacea (Bivalvia) of North America. *Malacologia*, *20*, 217–253.
De Queiroz, K. (2007). Species concepts and species delimitation. *Systematic Biology*, *56*, 879–886.
Eagar, R. M. C. (1950). Variation in shape of shell with respect to ecological station. A review dealing with Recent Unionidae and certain species of the Anthracosiidae in Upper Carboniferous times. *Proceedings of the Royal Society of Edinburgh: Section B. Biology*, *63*, 130–148.
Faircloth, B. C., McCormack, J. E., Crawford, N. G., Harvey, M. G., Brumfield, R. T., & Glenn, T. C. (2012). Ultraconserved elements anchor thousands of genetic markers spanning multiple evolutionary timescales. *Systematic Biology*, *61*, 717–726.
Fujita, M. K., Leaché, A. D., Burbrink, F. T., McGuire, J. A., & Moritz, C. (2012). Coalescent-based species delimitation in an integrative taxonomy. *Trends in Ecology & Evolution*, *27*, 480–488.
Gangloff, M. M., Williams, J. D., & Feminella, J. W. (2006). A new species of freshwater mussel (Bivalvia: Unionidae), *Pleurobema athearni*, from the Coosa River Drainage of Alabama, USA. *Zootaxa*, *1118*, 43–56.
Graf, D. L. (2013). Patterns of freshwater bivalve global diversity and the state of phylogenetic studies on the Unionoida, Sphaeriidae, and Cyrenidae. *American Malacological Bulletin*, *31*, 135–153.
Graf, D. L., & Cummings, K. S. (2006). Palaeoheterodont diversity (Mollusca: Trigonioida + Unionoida): What we know and what we wish we knew about freshwater mussel evolution. *Zoological Journal of the Linnean Society*, *148*, 343–394.
Graf, D. L., & Cummings, K. S. (2007). Review of the systematics and global diversity of freshwater mussel species (Bivalvia: Unionoida). *Journal of Molluscan Studies*, *73*, 291–314.
Grummer, J. A., Bryson, R. W., & Reeder, T. W. (2014). Species delimitation using Bayes factors: Simulations and application to the *Sceloporus scalaris* species group (Squamata: Phrynosomatidae). *Systematic Biology*, *63*, 119–133.
Haag, W. R. (2009). A hierarchical classification of freshwater mussel diversity in North America. *Journal of Biogeography*, *37*, 12–26.
Haag, W. R. (2012). *North American freshwater mussels: Natural history, ecology, and conservation*. Cambridge, UK: Cambridge University Press.
Haag, W. R., Warren, M. L., Wright, K., & Shaffer, L. (2002). Occurrence of the rayed creekshell, *Anodontoides radiatus*, in the Mississippi River Basin: Implications for conservation and biogeography. *Southeastern Naturalist*, *1*, 169–178.
Haag, W. R., & Williams, J. D. (2014). Biodiversity on the brink: An assessment of conservation strategies for North American freshwater mussels. *Hydrobiologia*, *735*, 45–60.
Hammer, Ø., Harper, D. A. T., & Ryan, P. D. (2001). PAST: Paleontological statistics software package for education and data analysis. *Palaeontologia Electronica*, *4*, 1–9.
Hillis, D. M., Pollock, D. D., McGuire, J. A., & Zwickl, D. J. (2003). Is sparse taxon sampling a problem for phylogenetic inference? *Systematic Biology*, *52*, 124–126.
Hoang, D. T., Chernomor, O., von Haeseler, A., Quang Minh, B., & Sy Vinh, L. (2018). Ufboot2: Improving the ultrafast bootstrap approximation. *Molecular Biology and Evolution*, *35*, 518–522.
Hoggarth, M. A. (1999). Descriptions of some of the glochidia of the Unionidae (Mollusca: Bivalvia). *Malacologia*, *41*, 1–118.
Hoggarth, M. A., & Gaunt, A. S. (1988). Mechanics of glochidial attachment (Mollusca: Bivalvia: Unionidae). *Journal of Morphology*, *198*, 71–81.
Howells, R. G., Neck, R. W., & Murray, H. D. (1996). *Freshwater Mussels of Texas*. Austin, TX: Texas Parks and Wildlife Press.
Hubbs, C. (1957). Distributional patterns of Texas freshwater fishes. *Southwestern Naturalist*, *2*, 89–104.
Hubbs, C., Edwards, R. J., & Garrett, G. P. (1991). An annotated checklist of freshwater fishes of Texas, with key to identification of species. *Texas Journal of Science*, *43*, 1–56.
Inoue, K., Hayes, D. M., Harris, J. L., & Christian, A. D. (2013). Phylogenetic and morphometric analyses reveal ecophenotypic plasticity in freshwater mussels *Obovaria jacksoniana* and *Villosa arkansasensis* (Bivalvia: Unionidae). *Ecology and Evolution*, *3*, 2670–2683.
Inoue, K., Hayes, D. M., Harris, J. L., Johnson, N. A., Morrison, C. L., Eackles, M. S., … Randklev, C. R. (2018). The Pleurobemini (Bivalvia: Unionida) revisited: Molecular species delineation using a mitochondrial DNA gene reveals multiple conspecifics and undescribed species. *Invertebrate Systematics*, *32*, 689–702.
Inoue, K., McQueen, A. L., Harris, J. L., & Berg, D. J. (2014). Molecular phylogenetics and morphological variation reveal recent speciation in freshwater mussels of the genera *Arcidens* and *Arkansia* (Bivalvia: Unionidae). *Biological Journal of the Linnean Society*, *112*, 535–545.
Iwata, H., & Ukai, Y. (2002). SHAPE: A computer program package for quantitative evaluation of biological shapes based on elliptic Fourier descriptors. *Journal of Heredity*, *93*, 384–385.
Johnson, N. A., Smith, C. H., Pfeiffer, J. M., Randklev, C. R., Williams, J. D., & Austin, J. D. (2018). Integrative taxonomy resolves taxonomic uncertainty for freshwater mussels being considered for protection under the U.S. Endangered Species Act. *Scientific Reports*, *8*, 15892.

Johnson, N., McLeod, J., Holcomb, J., Rowe, M., & Williams, J. (2016). Early life history and spatiotemporal changes in distribution of the rediscovered Suwannee moccasinshell *Medionidus walkeri* (Bivalvia: Unionidae). *Endangered Species Research*, *31*, 163–175.

Johnson, R. I. (1970). The systematics and zoogeography of the Unionidae (Mollusca: Bivalvia) of the southern Atlantic slope region. *Harvard University Museum Comparative Zoological Bulletin*, *140*, 263–450.

Jones, G. (2017). Algorithmic improvements to species delimitation and phylogeny estimation under the multispecies coalescent. *Journal of Mathematical Biology*, *74*, 447–467.

Jones, J. W., Neves, R. J., Ahlstedt, S. A., & Hallerman, E. M. (2006). A holistic approach to taxonomic evaluation of two closely related endangered freshwater mussel species, the oyster mussel *Epioblasma capsaeformis* and tan riffleshell *Epioblasma florentina walkeri* (Bivalvia: Unionidae). *Journal of Molluscan Studies*, *72*, 267–283.

Jordan, D. S. (1905). The origin of species through isolation. *Science (New York, N.Y.)*, *22*, 545–562.

Kalyaanamoorthy, S., Minh, B. Q., Wong, T. K. F., von Haeseler, A., & Jermiin, L. S. (2017). ModelFinder: fast model selection for accurate phylogenetic estimates. *Nature Methods*, *14*, 587–589.

Kass, R. E., & Raftery, A. E. (1995). Bayes factors. *Journal of the American Statistical Association*, *90*, 773–795.

Katoh, K., & Standley, D. M. (2013). MAFFT multiple sequence alignment software version 7: Improvements in performance and usability. *Molecular Biology and Evolution*, *30*, 772–780.

Kearse, M., Moir, R., Wilson, A., Stones-Havas, S., Cheung, M., Sturrock, S., … Drummond, A. (2012). Geneious Basic: An integrated and extendable desktop software platform for the organization and analysis of sequence data. *Bioinformatics*, *28*, 1647–1649.

King, T. L., Eackles, M. S., Gjetvaj, B., & Hoeh, W. R. (1999). Intraspecific phylogeography of *Lasmigona subviridis* (Bivalvia: Unionidae): Conservation implications of range discontinuity. *Molecular Ecology*, *8*, S65–S78.

Kishino, H., Miyata, T., & Hasegawa, M. (1990). Maximum likelihood inference of protein phylogeny and the origin of chloroplasts. *Journal of Molecular Evolution*, *31*, 151–160.

Kumar, S., Stecher, G., & Tamura, K. (2016). MEGA7: Molecular Evolutionary Genetics Analysis version 7.0 for bigger datasets. *Molecular Biology and Evolution*, *33*, 1870–1874.

Lanfear, R., Frandsen, P. B., Wright, A. M., Senfeld, T., & Calcott, B. (2016). PartitionFinder 2: New methods for selecting partitioned models of evolution for molecular and morphological phylogenetic analyses. *Molecular Biology and Evolution*, *34*, 772–773.

Lartillot, N., & Philippe, H. (2006). Computing Bayes factors using thermodynamic integration. *Systematic Biology*, *55*, 195–207.

Leaché, A. D., Zhu, T., Rannala, B., & Yang, Z. (2019). The spectre of too many species. *Systematic Biology*, *68*, 168–181.

Lefébure, T., Douady, C. J., Gouy, M., & Gibert, J. (2006). Relationship between morphological taxonomy and molecular divergence within Crustacea: Proposal of a molecular threshold to help species delimitation. *Molecular Phylogenetics and Evolution*, *40*, 435–447.

Leigh, J. W., & Bryant, D. (2015). POPART: Full-feature software for haplotype network construction. *Methods in Ecology and Evolution*, *6*, 1110–1116.

Lemmon, A. R., Emme, S. A., & Lemmon, E. M. (2012). Anchored hybrid enrichment for massively high-throughput phylogenomics. *Systematic Biology*, *61*, 727–744.

Lopes-Lima, M., Burlakova, L. E., Karatayev, A. Y., Mehler, K., Seddon, M., & Sousa, R. (2018). Conservation of freshwater bivalves at the global scale: Diversity, threats and research needs. *Hydrobiologia*, *810*, 1–14.

Lopes-Lima, M., Froufe, E., Do, V. T., Ghamizi, M., Mock, K. E., Kebapçı, Ü., … Bogan, A. E. (2017). Phylogeny of the most species-rich freshwater bivalve family (Bivalvia: Unionida: Unionidae): Defining modern subfamilies and tribes. *Molecular Phylogenetics and Evolution*, *106*, 174–191.

Maddison, W. P., & Maddison, D. R. (2017). Mesquite: A modular system for evolutionary analysis. Version 3.31. Retrieved from http://mesquiteproject.org. (accessed 23 June 2019)

Mayr, E. (1942). *Systematics and the origin species.* New York, NY: Columbia University Press.

Mayr, E. (1959). Isolation as an evolutionary factor. *Proceedings of the American Philosophical Society*, *103*, 221–230.

Mayr, E. (1963). *Animal species and evolution*. Cambridge, MA: Harvard University Press.

Moritz, C. (1994). Defining 'evolutionary significant units' for conservation. *Trends in Ecology and Evolution*, *9*, 373–375.

Nguyen, L.-T., Schmidt, H. A., von Haeseler, A., & Minh, B. Q. (2015). IQ-TREE: A fast and effective stochastic algorithm for estimating maximum-likelihood phylogenies. *Molecular Biology and Evolution*, *32*, 268–274.

Ogilvie, H. A., Bouckaert, R. R., & Drummond, A. J. (2017). StarBEAST2 brings faster species tree inference and accurate estimates of substitution rates. *Molecular Biology and Evolution*, *34*, 2101–2114.

Ortmann, A. E. (1920). Correlation of shape and station in fresh-water mussels (Naiades). *Proceedings of the American Philosophical Society*, *59*, 269–312.

Page, L. M., & Burr, B. M. (2011). *Peterson field guide to freshwater fishes of North America north of Mexico*. Boston, MA: Houghton Mifflin Harcourt.

Park, J.-K., & Foighil, D. Ó. (2000). Sphaeriid and corbiculid clams represent separate heterodont bivalve radiations into freshwater environments. *Molecular Phylogenetics and Evolution*, *14*, 75–88.

Perkins, M. A., Johnson, N. A., & Gangloff, M. M. (2017). Molecular systematics of the critically-endangered North American spinymussels (Unionidae: *Elliptio* and *Pleurobema*) and description of *Parvaspina* gen. nov. *Conservation Genetics*, *18*, 745–757.

Pfeiffer, J. M., Johnson, N. A., Randklev, C. R., Howells, R. G., & Williams, J. D. (2016). Generic reclassification and species boundaries in the rediscovered freshwater mussel '*Quadrula*' *mitchelli* (Simpson in Dall, 1896). *Conservation Genetics*, *17*, 279–292.

Pfeiffer, J. M., Sharpe, A. E., Johnson, N. A., Emery, K. F., & Page, L. M. (2018). Molecular phylogeny of the Nearctic and Mesoamerican freshwater mussel genus *Megalonaias*. *Hydrobiologia*, *811*, 139–151.

Pieri, A. M., Inoue, K., Johnson, N. A., Smith, C. H., Harris, J. L., Robertson, C., & Randklev, C. R. (2018). Molecular and morphometric analyses reveal cryptic diversity within

freshwater mussels (Bivalvia: Unionidae) of the western Gulf coastal drainages of the USA. *Biological Journal of the Linnean Society*, *124*, 261–277.
Pollock, D. D., Zwickl, D. J., McGuire, J. A., & Hillis, D. M. (2002). Increased taxon sampling is advantageous for phylogenetic inference. *Systematic Biology*, *51*, 664–671.
Rambaut, A., Drummond, A. J., Xie, D., Baele, G., & Suchard, M. A. (2018). Posterior summarization in Bayesian phylogenetics using Tracer 1.7. *Systematic Biology*, *67*, 901–904.
Ratnasingham, S., & Hebert, P. D. N. (2013). A DNA-based registry for all animal species: The Barcode Index Number (BIN) system. *Public Library of Science One*, *8*, e66213.
Roe, K. J., & Lydeard, C. (1998). Molecular systematics of the freshwater mussel genus *Potamilus* (Bivalvia: Unionidae). *Malacologia*, *39*, 195–205.
Roe, K. J., Simons, A. M., & Hartfield, P. (1997). Identification of a fish host of the inflated Heelsplitter *Potamilus inflatus* (Bivalvia: Unionidae) with a description of its glochidium. *American Midland Naturalist*, *138*, 48–54.
Ronquist, F., Teslenko, M., van der Mark, P., Ayres, D. L., Darling, A., Höhna, S., … Huelsenbeck, J. P. (2012). MrBayes 3.2: Efficient Bayesian phylogenetic inference and model choice across a large model space. *Systematic Biology*, *61*, 539–542.
Rozas, J., Ferrer-Mata, A., Sánchez-DelBarrio, J. C., Guirao-Rico, S., Librado, P., Ramos-Onsins, S. E., & Sánchez-Gracia, A. (2017). DnaSP 6: DNA Sequence Polymorphism analysis of large data sets. *Molecular Biology and Evolution*, *34*, 3299–3302.
Satler, J. D., Carstens, B. C., & Hedin, M. (2013). Multilocus species delimitation in a complex of morphologically conserved trapdoor spiders (Mygalomorphae, Antrodiaetidae, *Aliatypus*). *Systematic Biology*, *62*, 805–823.
Serb, J. M., Buhay, J. E., & Lydeard, C. (2003). Molecular systematics of the North American freshwater bivalve genus *Quadrula* (Unionidae: Ambleminae) based on mitochondrial ND1 sequences. *Molecular Phylogenetics and Evolution*, *28*, 1–11.
Shimodaira, H., & Hasegawa, M. (2001). CONSEL: For assessing the confidence of phylogenetic tree selection. *Bioinformatics (Oxford, England)*, *17*, 1246–1247.
Shimodaira, H. (2002). An approximately unbiased test of phylogenetic tree selection. *Systematic Biology*, *51*, 492–508.
Sietman, B. E., Hove, M. C., & Davis, J. M. (2018). Host attraction, brooding phenology, and host specialization on freshwater drum by 4 freshwater mussel species. *Freshwater Science*, *37*, 96–107.
Smith, C. H., Johnson, N. A., Pfeiffer, J. M., & Gangloff, M. M. (2018). Molecular and morphological data reveal non-monophyly and speciation in imperiled freshwater mussels (*Anodontoides* and *Strophitus*). *Molecular Phylogenetics and Evolution*, *119*, 50–62.
Smith, D. G. (2000). *Keys to the freshwater macroinvertebrates of southern New England*. Sunderland, MA: University of Massachusetts at Amherst. Department of Zoology.
Stiven, A., & Alderman, J. (1992). Genetic similarities among certain freshwater mussel populations of the *Lampsilis* genus in North Carolina. *Malacologia*, *34*, 355–369.
Strecker, J. K. (1931). *The distribution of the Naiades or pearly freshwater mussels of Texas*. Waco, TX: Baylor University Museum.
Sukumaran, J., & Knowles, L. L. (2017). Multispecies coalescent delimits structure, not species. *Proceedings of the National Academy of Sciences*, *114*, 1607–1612.
USFWS. (2009). Endangered and threatened wildlife and plants; 90-day finding on petitions to list nine species of mussels from Texas as threatened or endangered with critical habitat. *Federal Register*, *74*, 66260–66271.
Watters, G. T., Hoggarth, M. A., & Stansbery, D. H. (2009). *The freshwater mussels of Ohio*. Columbus, OH: Ohio State University Press.
Wickham, H. (2016). *ggplot2: Elegant graphics for data analysis.* New York, NY: Springer-Verlag.
Williams, J. D., Bogan, A. E., Butler, R. S., Cummings, K. S., Garner, J. T., Harris, J. L., … Watters, G. T. (2017). A revised list of the freshwater mussels (Mollusca: Bivalvia: Unionida) of the United States and Canada. *Freshwater Mollusk Biology and Conservation*, *20*, 33–58.
Williams, J. D., Bogan, A. E., & Garner, J. T. (2008). *Freshwater mussels of Alabama and the Mobile Basin in Georgia*. Tuscaloosa, AL: University of Alabama Press.
Williams, J. D., Butler, R. S., Warren, G. L., & Johnson, N. A. (2014). *Freshwater mussels of Florida*. Tuscaloosa, AL: University of Alabama Press.
Xia, X. (2018). DAMBE7: New and improved tools for data analysis in molecular biology and evolution. *Molecular Biology and Evolution*, *35*, 1550–1552.
Xia, X., Xie, Z., Salemi, M., Chen, L., & Wang, Y. (2003). An index of substitution saturation and its application. *Molecular Phylogenetics and Evolution*, *26*, 1–7.
Yang, Z., & Rannala, B. (2010). Bayesian species delimitation using multilocus sequence data. *Proceedings of the National Academy of Sciences*, *107*, 9264–9269.
Zanatta, D. T., & Murphy, R. W. (2006). Evolution of active host-attraction strategies in the freshwater mussel tribe Lampsilini (Bivalvia: Unionidae). *Molecular Phylogenetics and Evolution*, *41*, 195–208.
Zhang, C., Zhang, D.-X., Zhu, T., & Yang, Z. (2011). Evaluation of a Bayesian coalescent method of species delimitation. *Systematic Biology*, *60*, 747–761.
Zwickl, D. J., & Hillis, D. M. (2002). Increased taxon sampling greatly reduces phylogenetic error. *Systematic Biology*, *51*, 588–598.

Associate Editor: Andrea Waeschenbach